교육학석사학위논문

Real-time SERS Detection of Wound-induced Signals in Plants with PDDA-functionalized Bumpy Silver Nanoshells

PDDA로 싸여진 표면 증강 라만 산란 활성 은 나노 껍질을 이용한 식물체내 상처 유발 신호 실시간 검출에 관한 연구

2021년 2월

서울대학교 대학원

과학교육과 화학전공

신 동 욱

Real-time SERS Detection of Wound-induced Signals in Plants with PDDA-functionalized Bumpy Silver Nanoshells

지도교수 정 대 홍

이 논문을 교육학석사 학위논문으로 제출함

2021년 2월

서울대학교 대학원

과학교육과 화학전공

신 동 욱

신동욱의 교육학석사 학위논문을 인준함

2021 년 2 월

위 원 장 홍 훈 기 (인)

부위원장 정 대 홍 (인)

위 원 유 재 훈 (인)

Abstract

Real-time SERS Detection of Wound-induced Signals in Plants with PDDA-functionalized Bumpy Silver Nanoshells

Dong Uk Shin
Department of Science Education
(Major in Chemistry)
The Graduate School
Seoul National University

Real-time detection of phytohormones in the living plants is critical for understanding the plant defense response, and monitoring of growth conditions. Herein, poly(diallyldimethylammonium chloride) (PDDA)-functionalized bumpy silver nanoshells (AgNS@PDDA) were developed as surface-enhanced Raman scattering (SERS) nanoprobes that can detect phytohormones in plants. AgNS@PDDA represents high SERS enhancement, and NIR activity, so that the strong SERS intensity was

observed by the 785 nm photoexcitation. We obtained the distinctive SERS spectra of following three species with AgNS@PDDA: adenosine triphosphate (ATP), indole-3-acetic acid (IAA), and salicylic acid (SA), which can interact with PDDA through electrostatic attraction and hydrogen bonding. In watercress (*Nasturtium officinale*) leaf, AgNS@PDDA localized at the extracellular space of the mesophyll after infiltration through the stomata pores. We obtained the wound-induced SERS spectra of AgNS@PDDA in watercress leaf, and confirmed that three SERS peaks are correspond to the IAA with AgNS@PDDA Raman spectra. In addition, we demonstrate the potential application of real-time plant hormones detection by observing the increasing of IAA peaks over time from the wound-induced SERS spectra. These results indicate that the AgNS@PDDA is a highly sensitive nanosensors for use as a real-time monitoring plant defense responses.

Keyword : Surface-enhanced Raman Scattering (SERS), PDDA-functionalized silver bumpy nanoshells, electrostatic interaction, wound-induced signals, indole-3-acetic acid (IAA), real-time detection

Student Number : 2019-20603

Table of Contents

List of Figures

Chapter 1. Introduction

Plants recognize external stresses such as environmental changes or physical stimuli, and produce chemicals for propagation of specific signals as part of their defense system[1, 2]. Especially, wounding induces plant hormones such as jasmonic acid (JA), abscisic acid (ABA), salicylic acid (SA), ethylene (ET), and indole-3-acetic acid (IAA), which participate rapid cell-to-cell communication and affect the growth, differentiation and development of plants[3-5]. These chemicals interact with receptor protein on the cell surface and activate gene expression responsible to plant defense responses[6, 7]. Detection of wound-induced hormones is challenging because of their extremely low concentration of about micromolar level.

Recently, diagnostic techniques to monitor the chemicals in plants have drawn attention[8] because of rapid changes in growth conditions, which caused by global warming or the spread of insect pests. In particular, researchers have reported various approaches to detect plant hormones focused on surface-enhanced Raman scattering (SERS) owing to their unique optical characteristics[9]. High sensitivity of SERS probes enables assignment and detection of the plant hormones, despite of their low concentration. Various chemicals in plants have been assigned by SERS spectroscopy[10-13] and applied to determination of hormone levels in the whole plant[14]. However, most of reports suggested that SERS probes can be operate as nanosensors on the leaf surface[15, 16] or in the plants extraction[14, 17].

Tracking real-time reactions is difficult in the case of extraction, as well as detection of chemicals on the mesophyll cell surface through the SERS probes on the leaf. Therefore, overcoming limitations about SERS application in real-time in vivo detection of wound-induced plant hormones is required.

Herein, we develop the optical nanosensors that detect wound-induced SERS signals of plant defense responses (Figure 1). In the previous study, we have reported a seedless and surfactant-free synthetic method for silver bumpy nanoshells (AgNS)[18-20]. AgNS which surrounded by silver around the silica core has a multiple hot spots for highly enhanced Raman scattering because of their bumpy shell morphology[21]. We found that poly(diallyldimethyl-ammonium chloride) (PDDA)-functionalized silver bumpy nanoshells (AgNS@PDDA) attracts specific molecules to enter the local Raman hotspots and produce intense SERS signals when irradiated with 785 nm laser. We characterize the various properties of AgNS@PDDA, and evaluate to be suitable for signaling hormones in plants. Especially, selectively localization of AgNS@PDDA in leaf was confirmed by imaging with CLSM, and SERS intensity map of PDDA. The use of AgNS@PDDA allows for assignment of wound induced molecules related to plant defense pathways. These results indicate that the AgNS@PDDA have a great potential as multiplex detectable, and highly sensitive nanosensors for use as a real-time monitoring plant defense responses.

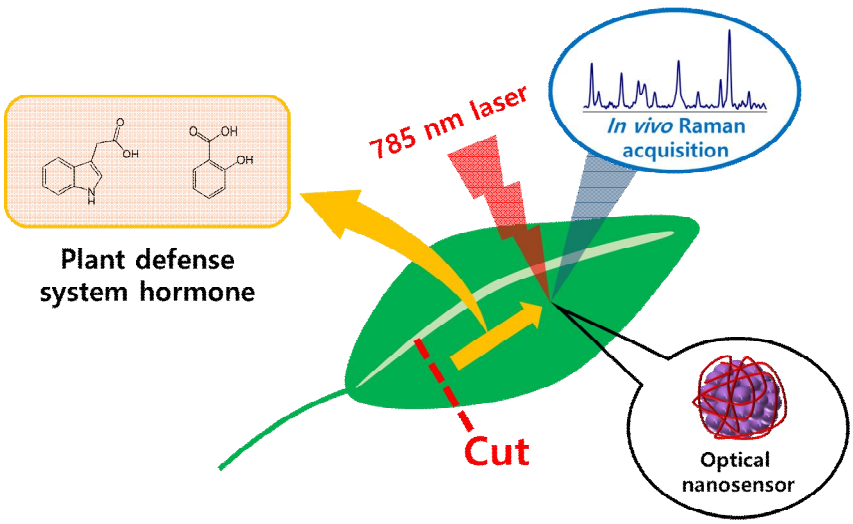

Figure 1. Schematic illustration of real-time in vivo SERS detection in plants using optical nanosensors. SERS spectrum of plants involve the information of plant defense responses.

Chapter 2. Experimental Section

2.1. Chemicals and Materials

Tetraethylorthosilicate (TEOS), ammonium hydroxide (NH_4OH, 28-30 %), 3-mercaptopropyl trimethoxysilane (MPTS), ethylene glycol (EG, spectrometric grade, > 99 %), silver nitrate ($AgNO_3$, > 99.99 %), hexadecylamine, 4-fluorothiophenol (4-FBT), poly(diallyldimethyl-ammonium chloride) solution (PDDA, average M_w < 100,000, 35 % in H_2O), adenosine 5'-triphosphate disodium salt hydrate (ATP), indole-3-acetic acid (IAA), salicylic acid (SA), 3-aminopropyl triethoxysilane (APTES), MES hydrate were purchased from Sigma-Aldrich (St. Louis, MO, USA) and used without further purification. Alexa Fluor 488 dye conjugated succinimidyl ester was purchased from Invitrogen (Carlsbad, CA, USA). Absolute ethanol (99.9 %), anhydrous ethanol (99 %), 2-propanol (99 %), magnesium sulfate anhydrous were purchased from Daejung Chemicals (Siheung, Korea). Deionized water was used for the whole experiment.

Watercress (*Nasturtium officinale*) was grown in a plant growth chamber at set condition of 60 % humidity, 22 ℃/18 ℃, medium light intensity, and 16 h light/8 h dark.

2.2. Instruments

The morphology of nanoparticles was observed using an energy-filtering transmission electron microscope (EF-TEM, LIBRA 120, Carl Zeiss). The absorption spectra of nanoparticles were measured using a UV-Vis spectrophotometer (UV-2600i, Shimadzu). The oxidation state and stability were measured using an X-ray photoelectron spectroscope (AXIS-His, KRAOTS). The size, homogeneity, concentration, and dispersity of nanoparticles were measured using a nanoparticle tracking analysis (NTA, LM10, Malvern Panalytical). The zeta potential values of nanoparticles were measured by Zeta-sizer Nano ZS90 (Malvern Instruments, UK). Confocal images were obtained using a confocal laser scanning microscope (CLSM, LSM 880 NLO, Carl Zeiss).

Raman signals of nanoprobes were measured using a confocal micro-Raman system (Xperam-200VN, Nanobase) equipped with an optical microscope (BX41M, Olympus). In this system, Raman signals were collected in a back scattering geometry and detected by a spectrometer equipped with a CCD detector (iDus 416, Andor, UK). The 785 nm laser (Leading-tech) was used as an excitation source. The excitation laser was focused and the Raman signals were collected using a x10 and x40 objective lens (NA 0.75, Olympus, Japan).

2.3. Preparation of AgNS@PDDA

The silica nanoparticles (SiNPs) were prepared by the Stöber method[22]. 1.6 mL of TEOS was dissolved in 40 mL of absolute ethanol (99.9 %) and 3 mL of ammonium hydroxide solution (28-30 %) was added. The reaction mixture was stirred vigorously for 20 h at 25 ℃. The synthesized SiNPs were centrifuged under 8,500 rpm for 15 min at 4 ℃ and washed with ethanol 5 times to remove excess reagents. The resulting SiNPs (~170 nm) were dispersed in ethanol to 50 mg/mL. Then, 50 μL of MPTS and 10 μL of ammonium hydroxide solution (28-30 %) was added to 1 mL of SiNPs for functionalized SiNPs surface with a thiol group. The mixture was shaken 12 h at 25 ℃. The thiol group functionalized SiNPs were centrifuged under 8,500 rpm for 10 min at 25 ℃ and washed with ethanol 5 times for purification. The resulting particles were dispersed in 1 mL of ethanol. Then, 60 μL of thiol group functionalized SiNPs was dissolved in 25 mL of ethylene glycol (EG), and 25 mL of 6 mM AgNO3 solution in ethylene glycol was added to reaction mixture. A 1 mL portion of hexadecylamine solution in ethanol was then rapidly added to the above solution (final concentration of hexadecylamine was 5 mM) and stirred vigorously for 1 h at 25 ℃. Synthesized silver bumpy nanoshells (AgNS) were centrifuged under 8,500 rpm for 15 min at 4 ℃ and washed with ethanol 5 times for purification. The resulting AgNS were dispersed in 3 mL of ethanol to 1 mg/mL. Then, 3 mL of AgNS were mixed with 27 mL of PDDA solution in

ethanol (final concentration of PDDA was 0.5 %) and stirred vigorously for 1h at 25 ℃. Then, PDDA functionalized AgNS (AgNS@PDDA) were centrifuged and washed with ethanol several times for purification. The resulting AgNS@PDDA were dispersed in 60 mL of ethanol to 0.05 mg/mL, purged with nitrogen gas and stored at 4 ℃.

2.4. Calculation of the SERS EF

SERS EF of the nanoprobes were calculated by the following equation:

$$EF = (I_{SERS} / I_{normal}) \div (N_{SERS} / N_{normal})$$

where I_{SERS} and I_{normal} are the intensity of the SERS and normal Raman scattering bands, respectively, N_{normal} and N_{SERS} are the number of 4-FBT molecules in normal form and self-assembled on the AgNS. 1075 cm^{-1} peak of 4-FBT Raman scattering bands was used to calculate the SERS EF. To label the 4-FBT to AgNS, 4-FBT was mixed with 1 mL of AgNS and incubated for 1h at 25 ℃. The mixture was centrifuged under 8,500 rpm for 5 min at 25 ℃ and washed with ethanol 2 times for purification. Each measurement was performed in a capillary tube using x10 objective lens with a 785 nm excitation, 5 mW laser power, and 5 sec acquisition time. Concentration of nanoprobes was measured by NTA, and averaging N_{SERS} of one AgNS was calculated by the following equation:

$$N_{SERS} \text{ of one AgNS} = 4\pi r^2 \div 2 \times r_f \div A_{4\text{-FBT}}$$

where r is the radius of the nanoprobes when its shape assumed complete spherical shape, r_f is the averaging roughness factor of AgNS, and $A_{4\text{-FBT}}$ is the area occupied by one 4-FBT molecule (0.383 nm^2/molecule). Excitation laser exposured area of AgNS assumed half of whole surface area.

2.5. SERS Measurement of Analytes with AgNS@PDDA

SERS measurement of adenosine triphosphate (ATP) and 2 kinds of each plant hormones (Indole-3-acetic acid, salicylic acid) were performed in a capillary tube. 1 mL of AgNS@PDDA were centrifuged and washed with water several times for purification. Each analytes was dissolved in mixture to 1 mM of final concentration, and sonicated for 10 sec. SERS spectra were measured 20 times using the confocal micro-Raman system with a 785 nm excitation, 10 mW laser power, and 10 sec acquisition time.

2.6. Preparation of Dye-conjugated Silica Nanoparticles

1.6 mL of TEOS was dissolved in 40 mL of absolute ethanol (99.9 %) and 2 mL of ammonium hydroxide solution (28-30 %) was added. The reaction mixture was stirred vigorously for 20 h at 25 ℃. The synthesized SiNPs were centrifuged under 8,500 rpm for 15 min at 4 ℃ and washed with ethanol 5 times to remove excess reagents. The resulting SiNPs (~250 nm) were dispersed in ethanol to 50 mg/mL. Then, 5 mg of SiNPs were dispersed in 1 mL of 2-propanol and 5 μL of APTES and 2 μL of ammonium hydroxide solution (28-30 %) was added to the mixture for functionalization of amino group on the surface of the SiNPs. This mixture was shaken 12 h at 25 ℃. APTES treated SiNPs were centrifuged under 8,500 rpm for 15 min at 4 ℃ and washed with 2-propanol 3 times, followed by washing with water 3 times. The resulting SiNPs were dispersed in 1 mL of water. In order to conjugate fluorescent dye to SiNPs, 27 μL of Alexa Flour 488 NHS ester (1 mg/mL) was added to 1 mL of APTES treated SiNPs, and stirred for 12 h at 25 ℃. The mixture was dialysed with a dialysis bag of 10kDa MWCO (-) for 3 days. Final AF488 conjugated SiNPs were dispersed in 10 mL of MES buffer (5 mM MES, 5 mM $MgSO_4$, pH 5.7) to 0.5 mg/mL.

2.7. Fluorescent Confocal Micrographs

AF488 conjugated SiNPs were infiltrated to the abaxial side of the watercress leaf using a needleless 1 mL syringe. During the infiltration, a sufficiently low pressure was applied to the leaf to ensure no mechanical damage was occurred. Then, abaxial side of SiNPs infiltrated leaf was washed with water to remove remained SiNPs on the surface. Confocal images were taken 1 hour after the infiltration of SiNPs. A leaf was cut using a scissors and prepare a wet mount slide with a cut leaf. Fluorescence images were split into AF488 and chlorophyll A channel using a x20 objective lens.

2.8. Detection of Wound-induced SERS Signals in Plants

AgNS@PDDA in MES buffer (5 mM MES, 5 mM $MgSO_4$, pH 5.7) were infiltrated to the abaxial side of the watercress leaf. Infiltration method is the same as SiNPs case. SERS measurements were taken 1 hour after the infiltration of AgNS@PDDA. Intact plant with roots in the MES buffer was used for the SERS measurement, and AgNS@PDDA injected leaf was fixed on the slide glass using a double-sided tape. Then, SERS measurement was performed within 100 μm of the inlet by point-by-point mapping with 1 μm step size using a x40 objective lens (0.65 NA, Olympus). Each experiments were carried out with a 785 nm excitation, 1 mW laser power, and 0.1 sec acquisition time.

Wound stress was performed by cutting the leaf using a scalpel. The cutting area was included the infiltrated region, and measurement was carried out within 100 μm of the wound. SERS spectra was obtained every 10 min after cutting using a x10 objective lens with a 785 nm excitation, 1 mW laser power, and 10 sec acquisition time.

Chapter 3. Results and Discussion

3.1. Synthesis and Characterization of AgNS@PDDA

AgNS@PDDA were prepared that can detect chemicals related plant defense system (Figure 2 (a)). Alkylamine plays roles the capping ligand and reducing agent simultaneously during the synthetic process of AgNS. It is known that hexadecylamine, which has long alkyl chains among alkylamines, produce the spiky shapes on the bumpy structures[23]. Figure 2 (b) shows the surface morphology of AgNS, and their bumpy shell structures enables formation of local hot spots. AgNS that synthesized using hexadecylamine exhibited high enhancement factor value (Figure 2 (c)) for 785 nm excitation owing to its spiky shapes. Then, PDDA was added to AgNS to prepare the AgNS@PDDA. PDDA stabilizes the surface charge of the AgNS and attracts the analyte molecules, allowing it to act as an optical nanosensors in plants.

To evaluate the AgNS@PDDA as the NIR sensitive SERS probe, the extinction spectrum of AgNS and AgNS@PDDA were obtained (Figure 3 (a)). AgNS synthesized using hexadecylamine has high plasmon resonance in the NIR region, and AgNS@PDDA maintain their NIR sensitivity. High extinction in the NIR region is proper for SERS detection in plants because the chlorophyll content of leaves emit strong fluorescence at 600-700 nm, so that the Raman signals are interfered with the fluorescence signals when 600-700 nm wavelength excitation laser is used. In this work, a 785 nm

laser that AgNS@PDDA has a high plasmonic response and receive minimal interference from the fluorescence of chlorophyll content was used as an excitation source.

In addition, the XPS analysis was performed right after synthesis of AgNS@PDDA and after storing at 4 ℃ for a week in water to evaluate the oxidation stability of AgNS@PDDA (Figure 3 (b)). The XPS spectrum of AgNS@PDDA shows not significant changes over time, and this results indicates that the AgNS@PDDA are not oxidized additionally in water. Oxidation of silver is a major factor in decreasing the enhancement factor of AgNS. High oxidation stability of AgNS@PDDA in water facilitates that the nanosensors operate for a long time after infiltration within the plants.

Next, the changes in hydrodynamic volume and zeta potential values were measured to confirm the capping of PDDA to the AgNS surface. The results of measuring the diameters and dispersity of AgNS and AgNS@PDDA through nanoparticle tracking analysis (NTA) are shown in figure 4 (a). AgNS@PDDA represents a larger diameter compared to AgNS, and it shows that AgNS is successfully functionalized with PDDA. A diameter of 304 nm suggested that AgNS@PDDA is a suitable for infiltration within the leafs through the stomata pores which their size is about 3 to 10 μm, however, it is large to enter within the mesophyll cell. We take this as evidence that AgNS@PDDA exists on the surface of leaf mesophyll cell, and these localization properties facilitates the detection of plant hormones in the extracellular space. Figure 4 (b) represents the

changes in surface charge of the AgNS after PDDA treatment. PDDA increases zeta potential of AgNS due to their positive charge of PDDA repeating unit. The high surface charge of about 45 mV indicates that the nanoprobes has sufficient dispersity, and affinity for molecules with negative charge.

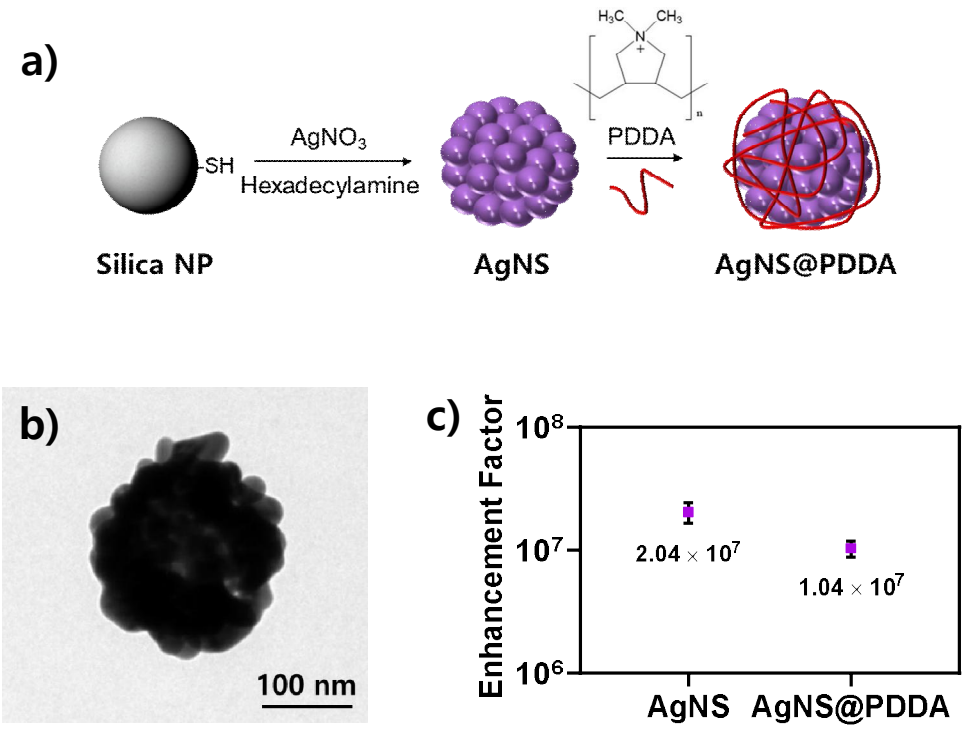

Figure 2. Preparation of AgNS@PDDA. (a) Schemes of synthetic process of AgNS@PDDA. (b) TEM image of AgNS@PDDA. (c) Enhancement factors of AgNS and AgNS@PDDA at 785 nm excitation laser.

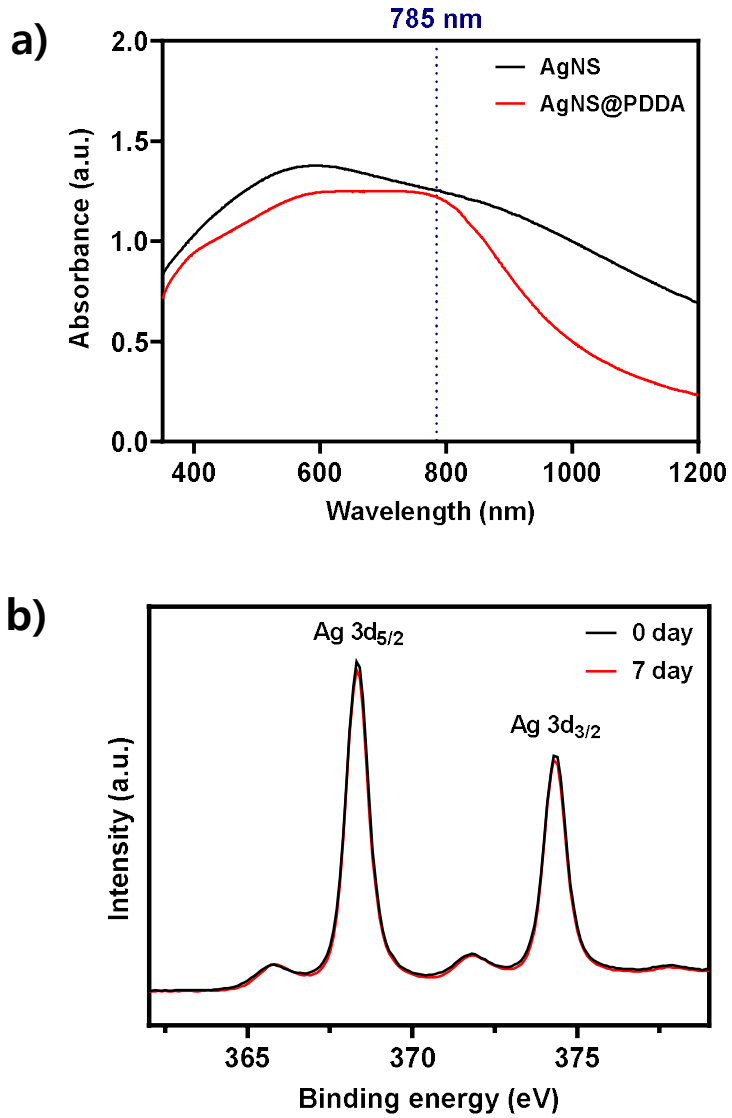

Figure 3. Characterization of AgNS and AgNS@PDDA. (a) UV-Vis spectra of AgNS and AgNS@PDDA. (b) XPS spectra of AgNS@PDDA. 368.3 eV and 374.3 eV peak indicates $3d_{5/2}$ and $3d_{3/2}$ of silver, respectively.

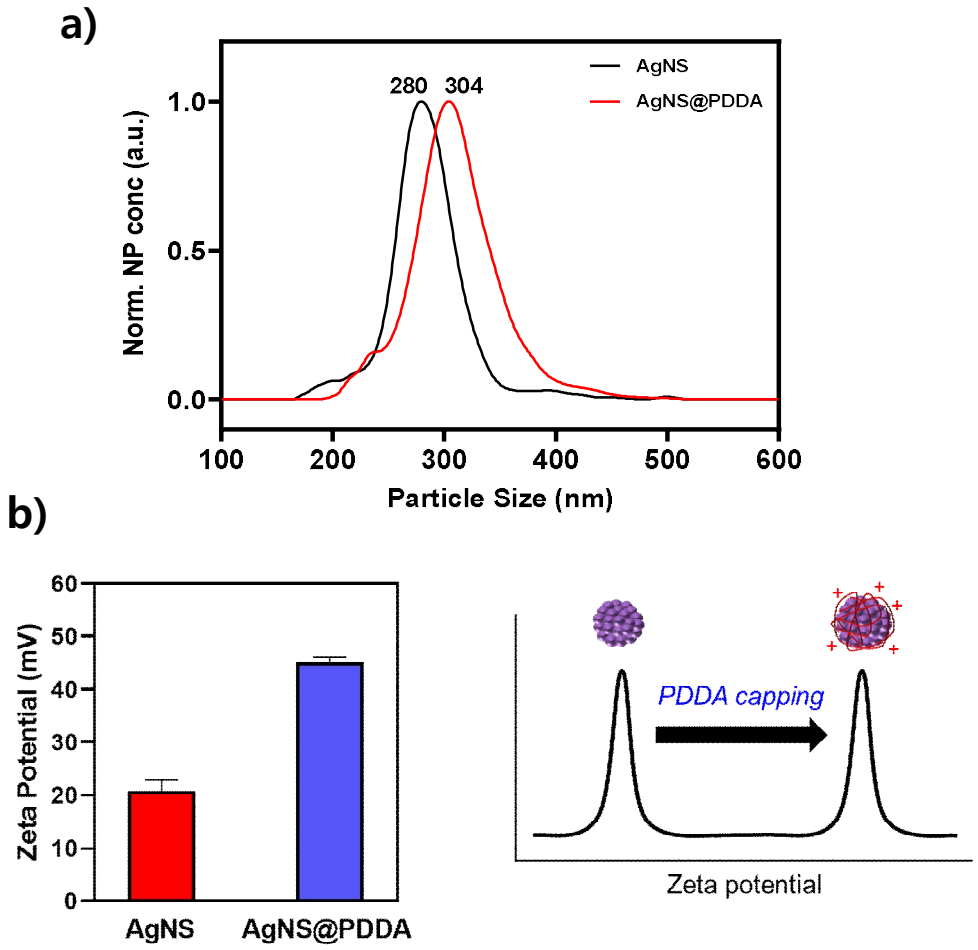

Figure 4. Capping of PDDA on the AgNS surface. (a) Size and distribution of AgNS and AgNS@PDDA measuring by nanoparticle tracking analysis (NTA). (b) Zeta potential values of AgNS and AgNS@PDDA. Each data was averages over 10 measurements.

3.2. Raman Enhancement Mechanism

Figure 5 (a) illustrates the Raman enhancement mechanism for detection of the target molecules with AgNS@PDDA. In this process, AgNS@PDDA interact with analyte molecules through the electrostatic interaction and hydrogen bonding. The high zeta potential of about 45 mV of PDDA produces electrostatic attraction with the negatively charged analyte molecules. Furthermore, PDDA is known to form a strong hydrogen bonding by formation of stacking structure with hydrogen bonding acceptor[24]. Whereas, the bare AgNS has no interaction with the analyte molecules, so that the negatively charged molecules not approach to the Raman hotspot and represents weak SERS intensity. To demonstrate the different SERS intensity of analyte molecules in AgNS and AgNS@PDDA, we measured the Raman signals in the water and adenosine triphosphate (ATP) solution, respectively. PDDA which exist at the Raman hotspots in AgNS@PDDA represents distinctive Raman band at 808 cm^{-1} as shown in Figure 5 (b). AgNS does not have a specific SERS peak in ATP solution, however, AgNS@PDDA has an intense SERS bands at the 730 cm^{-1} and 1331 cm^{-1}. Positive charge of PDDA attracts negatively charged phosphate group of ATP, and adenosine groups form hydrogen bonds with PDDA, resulting in ATP being present on the surface of AgNS@PDDA.

To demonstrate the utility of AgNS@PDDA as a plant optical nanosensors, SERS spectra of each three analytes (ATP, IAA, SA) were

obtained by the 785 nm photoexcitation. We select three analytes (Figure 6 (a)) that the most abundant chemicals when stress induced to plants. Since ATP exists in high concentration within the mesophyll cell[25], ATP diffuses when the cell is damaged and creates a local high level ATP environment. Stress also induces the indole-3-acetic acid (IAA)[7] and salicylic acid (SA)[26] which play roles the growth and development of plants. These analyte molecules also have a negatively charged functional group (ATP: triphosphate group, and IAA, SA: carboxylic group) at pH 5.7, so that these functional group form the electrostatic attraction with PDDA to approach the Raman hot spots. Furthermore, we observe an intense SERS signals of three analytes (ATP, IAA, SA) than other plant hormones (ABA, GA, JA) owing to their high Raman scattering cross sections. As shown in Fig 6 (b), ATP represents a specific SERS peaks at 730 cm^{-1} and 1330 cm^{-1} that assigned the vibration of adenine group[24]. SERS peaks of IAA that one of the indole derivatives was measured at 759 cm^{-1} and 1355 cm^{-1} indicating the indole ring vibration[27]. We observe the particularly intense SERS peaks at 806 cm^{-1} and other six peaks of SA as shown in Figure 6 (b)[28].

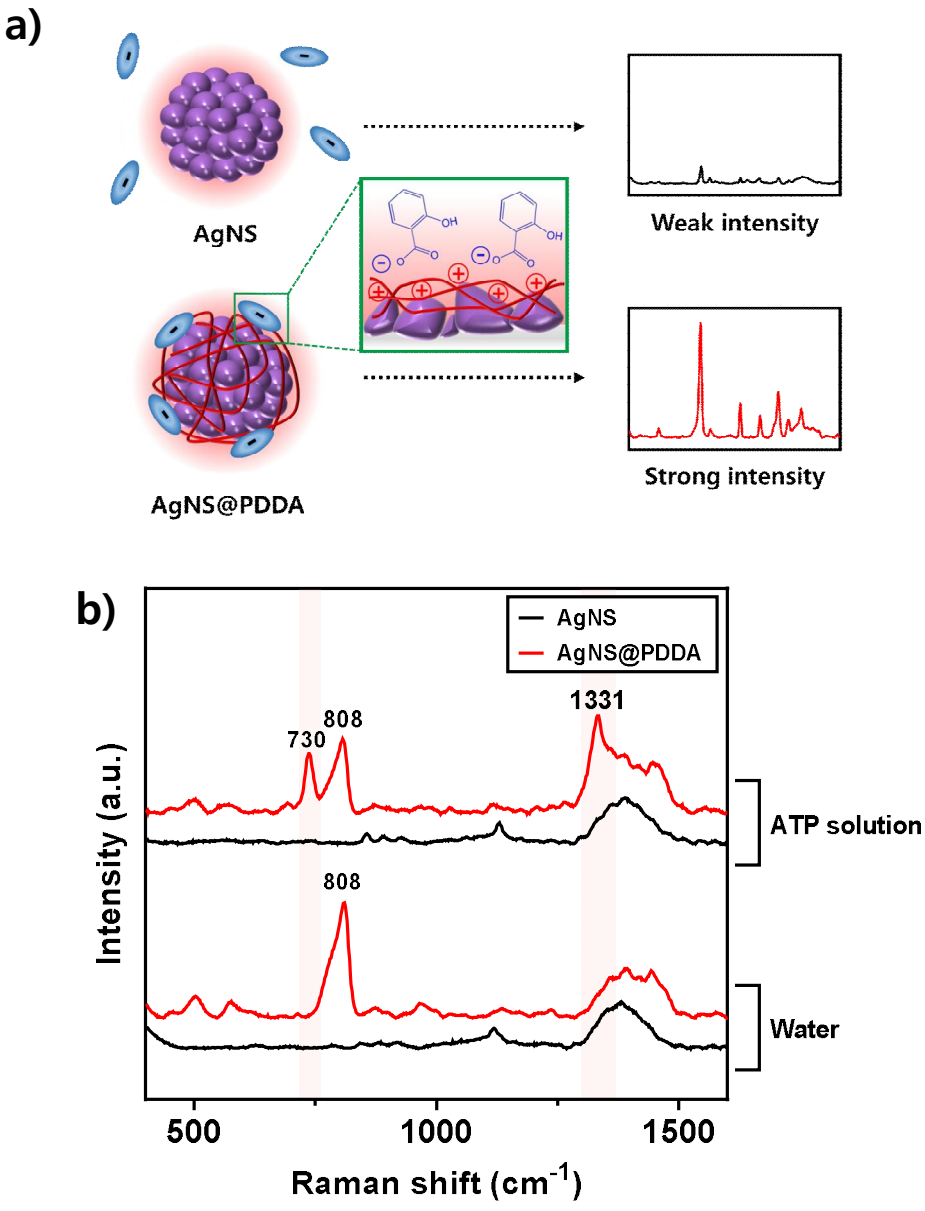

Figure 5. Interaction between PDDA and analyte molecules. (a) Schematic illustration for the electrostatic interaction of AgNS@PDDA with negatively charged molecules in the Raman hotspots. (b) SERS spectra of AgNS and AgNS@PDDA in water and ATP 10 μM solution.

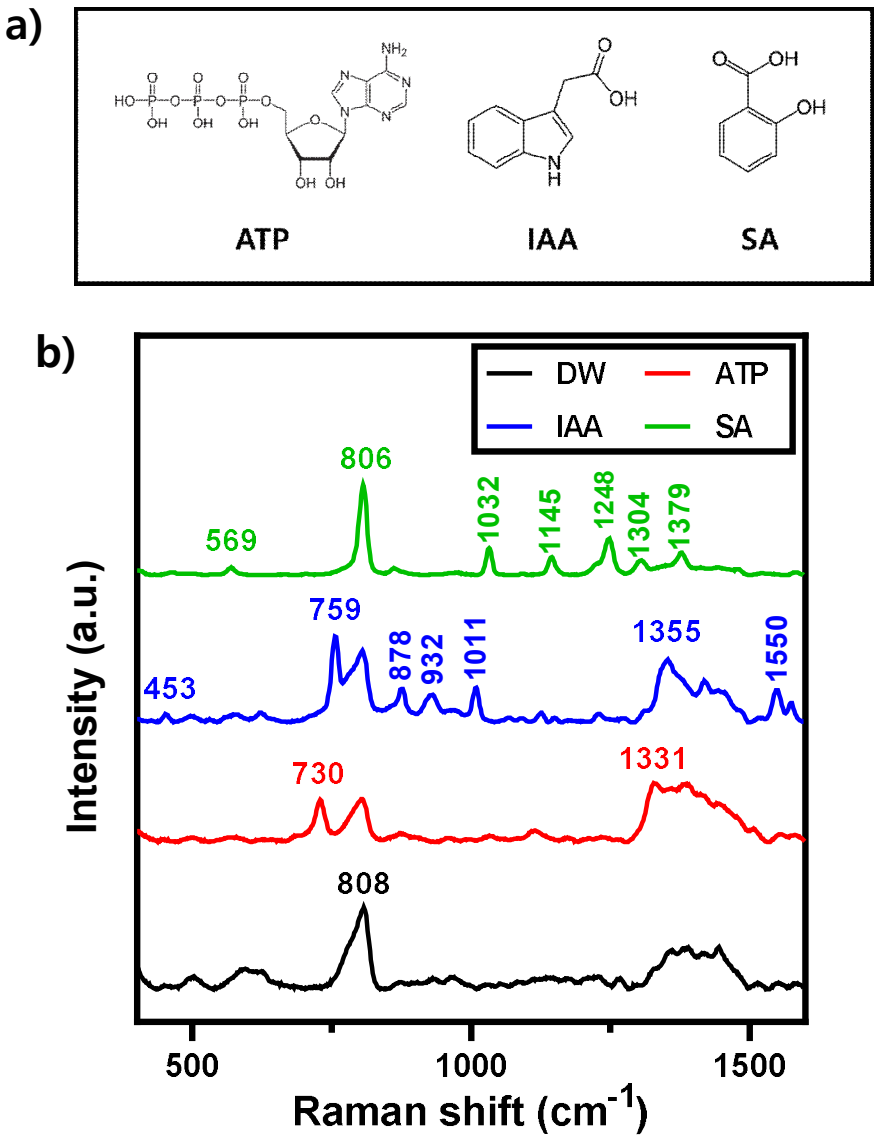

Figure 6. SERS peak assignment of three analytes with AgNS@PDDA. (a) Chemical structures of analytes: ATP, IAA, SA. (b) SERS spectrum of each analytes with AgNS@PDDA. Concentration of analytes was 1 mM, and SERS spectra were obtained by the 785 nm photoexcitation with a 10 mW laser power and 10 s light acquisition time except SA (1s).

3.3. Fluorescent Confocal Imaging of Nanoprobes in Plants

Distribution of nanoparticles in leaf was confirmed by using fluorescent confocal microscopy (Figure 7). Silica nanoparticles conjugated with Alexa Fluor 488 (SiNP-AF488) are observed in leaf epidermis cell and extracellular spaces of mesophyll of watercress plant. SiNP-AF488 of 250 nm diameter has been entered through the stomatal pores on the abaxial sides and localized to mesophyll cell surface. This results are consistent with our discussion of NTA data that the nanoprobes of 300 nm will not enter the intercellular spaces of mesophyll cell as shown in Figure 4 (a). In addition, we observe that SiNP-AF488 also presents on the surface of epidermis cell and the depth of epidermis is near 10 μm. Since the fluorescence of chlorophyll content and the passage of cytoplasm, the deeper the focal depth goes from the surface of abaxial side, the more scattering occurs and the Raman intensity becomes weaker. In this work, SERS signals were measured at a depth of 5 μm from the abaxial surface to obtain the information of mesophyll cell and maximal SERS intensity.

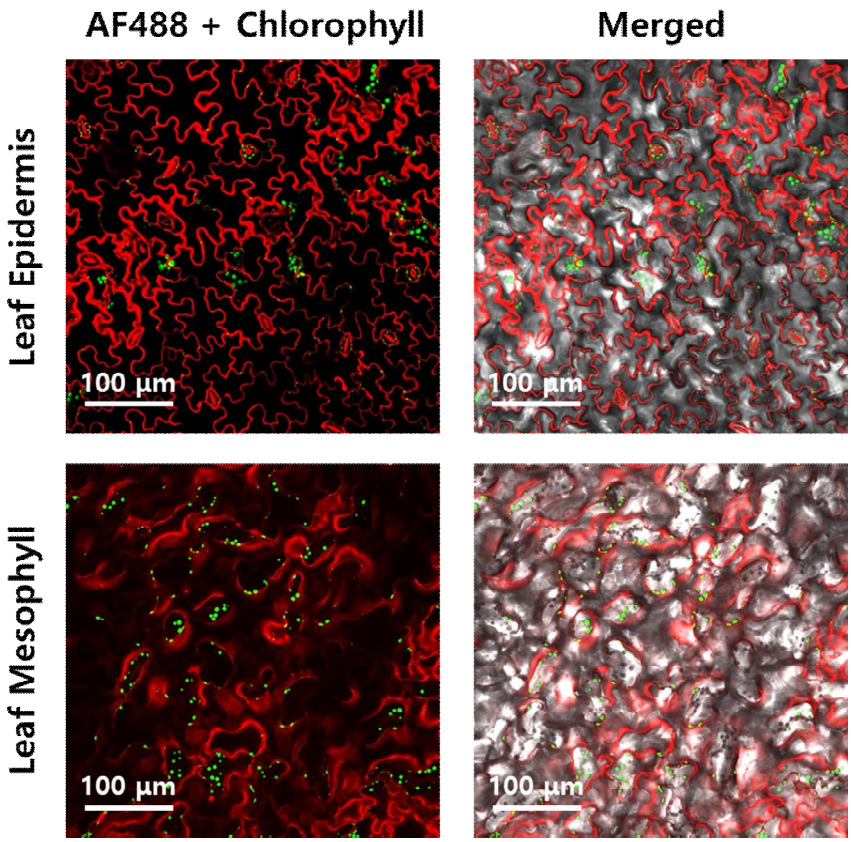

Figure 7. Fluorescent confocal images of dye-conjugated silica nanoparticles (SiNP-AF488, red) and chloroplast (Chlorophyll A, green) in the watercress leaf. Bright field images are merged right side.

3.4. Detection of Wound-induced SERS Signals in Plants

AgNS@PDDA were infiltrated to the abaxial side of the watercress leaf using a needleless 1 mL syringe, and SERS signals were measured after 1 hour. The watercress leaf locally wet at the moment of infiltration, and completely dry after 1 hour as shown in Figure 8 (a). Optical images after the infiltration shows that mechanical damages not occurred during the infiltration. Then, we obtain the SERS intensity map of AgNS@PDDA in watercress leaf using a micro-Raman system with 785 nm photoexcitation (Figure 8 (b)). The roots of watercress plant were submerged in 10 mM $MgSO_4$ solution and AgNS@PDDA infiltrated leaf was fixed on the slide glass using a double-sided tape. Figure 8 (c) shows the representative Raman mapping data of the strongest PDDA signal at 808 cm^{-1} in watercress leaf. SERS was measured using point-by-point mapping using with a step size of 1 μm, an integration time of 0.1 sec, and an excitation of 785 nm. We demonstrate that the AgNS@PDDA localizes at the mesophyll cell surface from the distribution of PDDA signals in the Raman intensity map, as well as shown in Figure 7. In addition, this results suggest that the AgNS@PDDA probes can be used for in vivo detection of target plant molecules and SERS mapping of plant hormones.

Finally, we obtained the SERS spectra of wound-induced watercress plants to demonstrate the potential applicability of AgNS@PDDA as optical nanoprobes. We cut the leaf into a square size of 2 cm around the infiltration

region using scalpel, and observed the SERS signals using a x40 objective lens. Figure 9 (a) represents that the spectra have a several specific SERS peaks including the signal from PDDA at 808 cm^{-1}. Among them, the peaks seen in 453 cm^{-1}, 759 cm^{-1}, 1359 cm^{-1} correspond to the SERS signals of the IAA with AgNS@PDDA (Figure 6 (b)). A large body of prior work[29, 30], suggesting IAA induced by their wound response, supports this results. Research has shown that IAA involved in growth and development of plants, and play major roles in plant defense system. Real-time SERS measurement was also employed to confirm the increasing IAA signals over time. The cutting area was included the infiltrated region, and measurement was carried out within 100 μm of the wound. The SERS spectra was obtained every 10 minutes (Figure 9 (b)), and this results indicates that the IAA signals increase over time. These demonstrations illustrate the potential for real-time in vivo detection of plant defense system hormones using AgNS@PDDA.

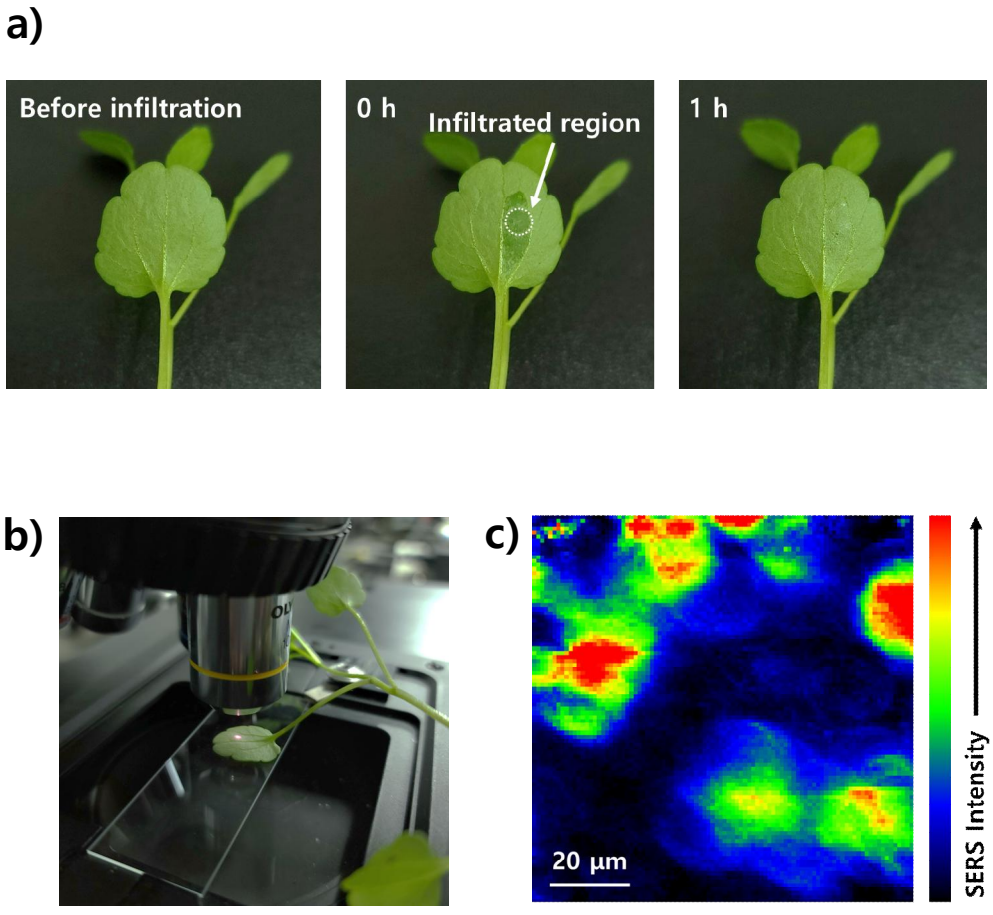

Figure 8. In vivo detection of the AgNS@PDDA in plants. (a) Images of the AgNS@PDDA introduction into living watercress plants. (b) Photograph of the Raman measurement setup for in vivo SERS detection. (c) SERS intensity map of 808 cm^{-1} peak of AgNS@PDDA in the watercress leaf.

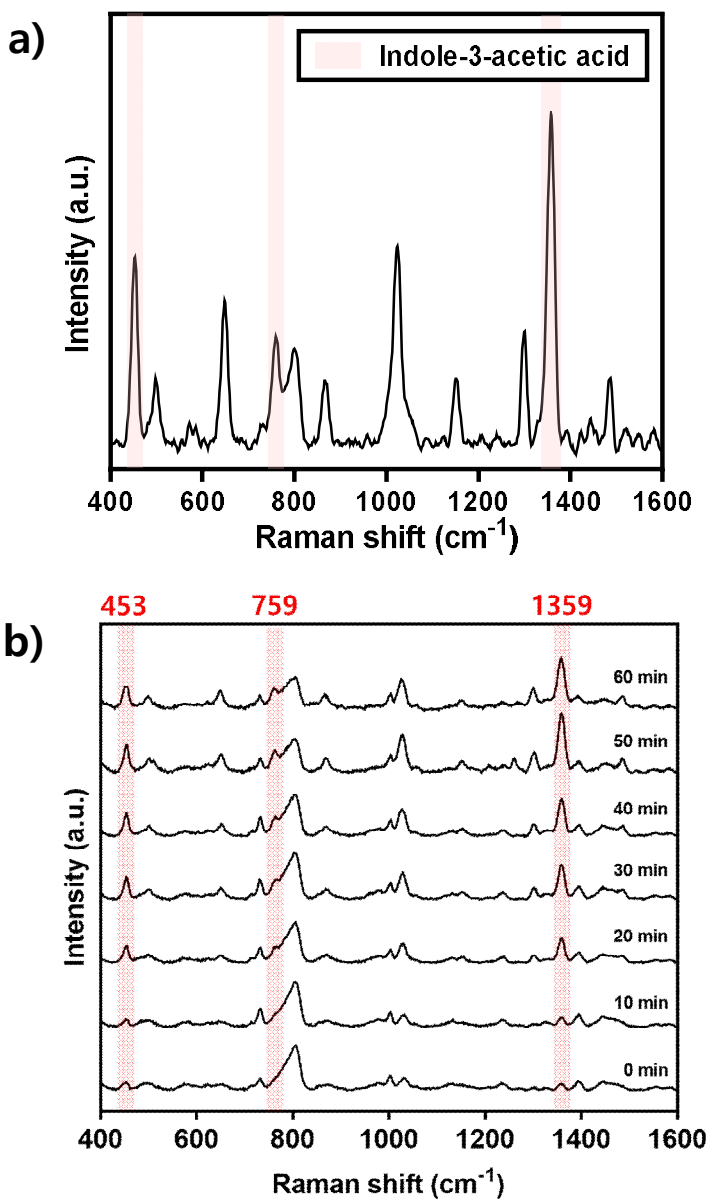

Figure 9. Detection of wound-induced SERS signals in AgNS@PDDA infiltrated plants. (a) Wound-induced SERS signals of the cutting leaf. (b) Real-time SERS detection at the 100 μm from the wound site. Each spectrum was obtained by the 785 nm photoexcitation with a 1 mW laser power and 10 s light acquisition time.

Chapter 4. Conclusion

In summary, we show that AgNS@PDDA can perform as optical nanosensors in plants. To detect the molecules related to the plant defense system, we designed PDDA-functionalized AgNS which can attract the target molecules through the electrostatic interaction and hydrogen bonding. PDDA capping is confirmed by increasing zeta potential, hydrodynamic volume, and specific SERS peak at 808 cm^{-1}. AgNS@PDDA is suitable for sensing of plant hormones in leaf because of its high oxidation stability, NIR sensitivity, and enhancement factor. This optical nanosensor can detect the chemicals in plants such as AT, IAA, or SA. AgNS@PDDA localizes at the leaf mesophyll cell surface, and it confirmed by fluorescence confocal image and SERS mapping of PDDA peaks at 808 cm^{-1}. Then, we obtain the SERS spectra in wound-induced leaf that match with the IAA Raman spectra with AgNS@PDDA. This results suggest that wounding induces IAA which involved in growth of plants from the SERS spectra of cutting plants. Given its potential use demonstrated here, AgNS@PDDA can be applied to real-time in vivo detection of plant defense system hormones.

Our techniques of observing SERS using the optical nanosensor in plants can be utilized in the basic studies of the plant defense system and molecular interaction with nanosensor. Infiltration of nanosensors within living plants that used in our study is non-destructive method and enables real-time detection at the molecular level. In addition, nanosensors can

introduced within specific spot, and sensor system operates as soon as introduced. Our study can potentially extend to establish analysis system of plant defense responses caused by changes in growth conditions.

5. References

1. Hedrich, R.;Salvador-Recatala, V.Dreyer, I., Electrical Wiring and Long-Distance Plant Communication. *Trends. Plant. Sci.* **2016**, 21(5), 376-387.

2. Spoel, S. H.Dong, X., How Do Plants Achieve Immunity? Defence without Specialized Immune Cells. *Na.t Rev. Immunol.* **2012**, 12(2), 89-100.

3. Savatin, D. V.;Gramegna, G.;Modesti, V.Cervone, F., Wounding in the Plant Tissue: The Defense of a Dangerous Passage. *Front. Plant. Sci.* **2014**, 5(470).

4. Toyota, M.;Spencer, D.;Sawai-Toyota, S.;Jiaqi, W.;Zhang, T.;Koo, A. J.;Howe, G. A.Gilroy, S., Glutamate Triggers Long-Distance, Calcium-Based Plant Defense Signaling. *Science.* **2018**, 361(6407), 1112-1115.

5. Lew, T. T. S.;Koman, V. B.;Silmore, K. S.;Seo, J. S.;Gordiichuk, P.;Kwak, S. Y.;Park, M.;Ang, M. C.;Khong, D. T.;Lee, M. A.;Chan-Park, M. B.;Chua, N. H.Strano, M. S., Real-Time Detection of Wound-Induced H_2O_2 Signalling Waves in Plants with Optical Nanosensors. *Nat. Plants.* **2020**, 6(4), 404-415.

6. Blazquez, M. A.;Nelson, D. C.Weijers, D., Evolution of Plant Hormone Response Pathways. *Annu. Rev. Plant. Biol.* **2020**, 71, 327-353.

7. Leyser, O., Auxin Signaling. *Plant. Physiol.* **2018**, 176(1), 465-479.

8. Kwak, S. Y.;Wong, M. H.;Lew, T. T. S.;Bisker, G.;Lee, M. A.;Kaplan, A.;Dong, J. Y.;Liu, A. T.;Koman, V. B.;Sinclair, R.;Hamann, C.Strano, M. S., Nanosensor Technology Applied to Living Plant Systems. *Annu. Rev.* **2017**, 10, 113-140.

9. Du, S. Y.;Yu, C. D.;Tang, L.Lu, L. X., Applications of SERS in the Detection of Stress-Related Substances. *Nanomaterials.* **2018**, 8(10).

10. Talian, I.;Oriňák, A.;Efremov, E. V.;Ariese, F.;Kaniansky, D.;Oriňáková, R.Hübner, J., Detection of Biologically Active Diterpenoic Acids by Raman Spectroscopy. *J. Raman. Spectrosc.* **2010**, 41(9), 964-968.

11. Castro, J. L.;Arenas, J. F.;Lopez-Ramirez, M. R.;Pelaez, D.Otero, J. C., Surface-Enhanced Raman Scattering of Hydroxybenzoic Acids Adsorbed on Silver Nanoparticles. *J. Colloid. Interface. Sci.* **2009**, 332(1), 130-135.

12. Tu, Q. A.;Eisen, J.Chang, C., Surface-Enhanced Raman Spectroscopy Study of Indolic Molecules Adsorbed on Gold Colloids. *J. Biomed. Opt.* **2010**, 15(2).

13. Zhang, P.;Wang, L. M.;Zheng, D. W.;Lin, T. F.;Wei, X. D.;Liu, X. Y.Wang, H. Q., Surface-Enhanced Raman Spectroscopic Analysis of N-6-Benzylaminopurine Residue Quantity in Sprouts with Gold Nanoparticles. *J. Environ. Sci. Health. B.* **2018**, 53(9), 561-566.

14. Wang, F.;Gu, X.;Zheng, C.;Dong, F.;Zhang, L.;Cai, Y.;You, Z.;You, J.;Du, S.Zhang, Z., Ehrlich Reaction Evoked Multiple Spectral Resonances and Gold Nanoparticle Hotspots for Raman Detection of Plant Hormone. *Anal. Chem.* **2017**, 89(17), 8836-8843.

15. Hou, R.;Pang, S.He, L., In Situ SERS Detection of Multi-Class Insecticides on Plant Surfaces. *Anal. Methods.* **2015**, 7(15), 6325-6330.

16. Zeiri, L., SERS of Plant Material. *J. Raman. Spectrosc.* **2007**, 38(7), 950-955.

17. Chen, M.;Zhang, Z. M.;Liu, M. Z.;Qiu, C.;Yang, H.Chen, X. Q., In

Situ Fabrication of Label-Free Optical Sensing Paper Strips for the Rapid Surface-Enhanced Raman Scattering (SERS) Detection of Brassinosteroids in Plant Tissues. *Talanta.* **2017**, 165, 313-320.

18. Chang, H.;Kang, H.;Yang, J. K.;Jo, A.;Lee, H. Y.;Lee, Y. S.Jeong, D. H., Ag Shell-Au Satellite Hetero-Nanostructure for Ultra-Sensitive, Reproducible, and Homogeneous NIR SERS Activity. *ACS. Appl. Mater. Interfaces.* **2014**, 6(15), 11859-11863.

19. Kang, H.;Yang, J. K.;Noh, M. S.;Jo, A.;Jeong, S.;Lee, M.;Lee, S.;Chang, H.;Lee, H.;Jeon, S. J.;Kim, H. I.;Cho, M. H.;Lee, H. Y.;Kim, J. H.;Jeong, D. H.Lee, Y. S., One-Step Synthesis of Silver Nanoshells with Bumps for Highly Sensitive near-IR SERS Nanoprobes. *J. Mater. Chem. B.* **2014**, 2(28), 4415-4421.

20. Yang, J. K.;Kang, H.;Lee, H.;Jo, A.;Jeong, S.;Jeon, S. J.;Kim, H. I.;Lee, H. Y.;Jeong, D. H.;Kim, J. H.Lee, Y. S., Single-Step and Rapid Growth of Silver Nanoshells as SERS-Active Nanostructures for Label-Free Detection of Pesticides. *ACS. Appl. Mater. Interfaces.* **2014**, 6(15), 12541-12549.

21. Chang, H.;Ko, E.;Kang, H.;Cha, M. G.;Lee, Y.-S.Jeong, D. H., Synthesis of Optically Tunable Bumpy Silver Nanoshells by Changing the Silica Core Size and Their SERS Activities. *RSC. Adv.* **2017**, 7(64), 40255-40261.

22. Werner, S.;Arthur, F.Ernst, B., Controlled Growth of Monodisperse Silica Spheres in the Micron Size Range. *J. Colloid. Interface. Sci.* **1968**, 26, 62-69.

23. Cha, M. G.;Kang, H.;Choi, Y. S.;Cho, Y.;Lee, M.;Lee, H. Y.;Lee, Y. S.Jeong, D. H., Effect of Alkylamines on Morphology Control of Silver Nanoshells for Highly Enhanced Raman Scattering. *ACS. Appl. Mater. Interfaces.* **2019**, 11(8), 8374-8381.

24. Lv, W.;Liu, C.;Ma, Y.;Wang, X.;Luo, J.Ye, W., Multi-Hydrogen Bond Assisted Sers Detection of Adenine Based on Multifunctional Graphene Oxide/Poly (Diallyldimethyl Ammonium Chloride)/Ag Nanocomposites. *Talanta.* **2019**, 204, 372-378.

25. Hoefnagel, M. H. N.;Atkin, O. K.Wiskich, J. T., Interdependence between Chloroplasts and Mitochondria in the Light and the Dark. *Biochim. Biophys. Acta.* **1998**, 1366(3), 235-255.

26. Vlot, A. C.;Dempsey, D. A.Klessig, D. F., Salicylic Acid, a Multifaceted Hormone to Combat Disease. *Annu. Rev. Phytopathol.* **2009**, 47, 177-206.

27. Razmute-Razme, I.;Kuodis, Z.;Olegas, E. L.Niaura, G., In-Situ Surface-Enhanced Raman Spectroscopic Investigation of NH Site of Indole Ring-Terminated Self-Assembled Monolayer on Gold Electrode. *Chemija.* **2007**, 18(4), 16-20.

28. Castro, J. L.;Arenas, J. F.;Lopez-Ramirez, M. R.Otero, J. C., Detecting Photoinduced Electron Transfer Processes in the Sers Spectrum of Salicylate Anion Adsorbed on Silver Nanoparticles. *Biopolymers.* **2006**, 82(4), 379-383.

29. Aloni, R.;Aloni, E.;Langhans, M.Ullrich, C. I., Role of Cytokinin and Auxin in Shaping Root Architecture: Regulating Vascular Differentiation, Lateral Root Initiation, Root Apical Dominance and Root Gravitropism. *Ann. Bot.* **2006**, 97(5), 883-893.

30. Chen, L. Q.;Tong, J. H.;Xiao, L. T.;Ruan, Y.;Liu, J. C.;Zeng, M. H.;Huang, H.;Wang, J. W.Xu, L., Yucca-Mediated Auxin Biogenesis Is Required for Cell Fate Transition Occurring During De Novo Root Organogenesis in Arabidopsis. *J. Exp. Bot.* **2016**, 67(14), 4273-4284.

국문 초록

살아있는 식물로부터 호르몬을 실시간 검출하는 것은 식물 방어 체계를 이해하고 식물의 생장 조건을 모니터링하는 관점에서 매우 중요하다. 우리는 이번 연구에서 식물 내 호르몬을 검출할 수 있는 표면 증강 산란 (Surface-enhanced Raman scattering) 나노프로브인 PDDA로 싸여진 은 나노 껍질 (AgNS@PDDA)를 개발하였다. AgNS@PDDA는 높은 SERS 증강과 NIR 활성을 나타내므로 785 nm의 들뜸 레이저로부터 강한 SERS 세기를 나타낸다. 우리는 AgNS@PDDA와 함께 PDDA와 정전기적 인력과 수소 결합으로 상호작용할 수 있는 세 가지 물질 (ATP, IAA, SA)에 대해 각각의 특징적인 SERS 스펙트럼을 얻었다. 물냉이의 잎으로 들어간 AgNS@PDDA는 주로 해면 조직 세포의 바깥 공간에 위치한다. 물냉이의 잎에 상처를 유발하여 얻은 SERS 스펙트럼에서는 세 개의 봉우리가 AgNS@PDDA와 함께 측정한 IAA의 봉우리들과 일치하는 것을 확인하였다. 더불어 우리는 상처 유발 SERS 스펙트럼으로부터 IAA의 신호가 시간에 따라 점점 증가하는 것을 관찰하여 식물 호르몬의 실시간 검출에 대한 적용 가능성을 입증하였다. 이 결과들은 AgNS@PDDA가 식물 방어체계를 실시간 모니터링할 수 있는 고감도의 나노센서로 활용될 수 있음을 보여준다.

주요어 : 표면 증강 라만 산란 (SERS), PDDA 로 싸여진 은 나노 껍질, 정전기적 상호작용, 상처 유발 신호, 인돌-3-아세트산 (IAA), 실시간 검출

학번 : 2019-20603